UNIVERSITY OF WEST BOHEMIA

Applied and Computational Mechanics 4 (2010) 49–56

Applied and Computational Mechanics

# Prediction of brittle fracture of epoxy-aluminum flanging

J. Korbel[a,b,*], L. E. Schmidt[a], B. Singh [a], N. Zant[a], J. Klusák[b], Z. Knésl[b]

[a] *ABB Switzerland Ltd, Corporate Research, 5405 Baden-Daettwil, Switzerland*
[b] *Ústav fyziky materiálů AV ČR, Žizkova 22, 616 62 Brno, Czech Republic*

Received 12 October 2009; received in revised form 21July 2010

**Abstract**

This paper presents a fracture mechanical approach for estimation of critical bending load of different types of aluminum-epoxy flanging and comparison with experimental measurements. For this purpose, several designs of the flanges were investigated. The flanges were glued to the epoxy bars and adhesive-epoxy interface was considered as a bi-material notch. Prediction of the failure is based on generalized stress intensity factor and generalized fracture toughness.


*Keywords:* generalized stress intensity factor, flanging, FEM, bi-material interface, fracture mechanics

## 1. Introduction

Metal-epoxy flanging is a common fastening method in electro technical industry. The main reason for using insulating materials (epoxy resin, polymer concrete, polyurethane, etc.) is for their dielectric properties. However, structures made of insulating material (bushings, spacers, fuse cutouts, etc.) have to transmit mechanical load as well. Prediction of the failure of brittle materials, such as epoxy resins, is well known theory and it is usually based on maximal principal or equivalent stress. In some specific cases the evaluation of the mechanical failure is not so simple. Instead of stress based failure criterions, fracture mechanical approach have to be used. In this contribution we applied a fracture mechanical approach in order to determine critical bending loading for various designs of the aluminum flange glued to the epoxy bar.

## 2. Materials and sample preparation

The investigated material was a standard epoxy formulation used for outdoor insulation purpose. The constituents are listed in Table 1. The raw materials were preheated to $65\,^{\circ}$C prior to mixing. The mixing was carried out in a batch mixer until a homogenous mixture was obtained. The blend was then degassed at a pressure of 5 mbar and cast into the tube moulds, having an inner diameter of 20 mm. The moulds were put in a forced convection oven for 2 h at $90\,^{\circ}$C for curing and 10 h at $140\,^{\circ}$C for postcuring. The epoxy rods were demoulded, and machined at the rods' ends to remove the top-layer of epoxy containing release agent. This step is necessary to ensure proper bonding between epoxy rod and flange. The adhesive used for bonding was the 2 component glue AV138M-HV998 also supplied from Huntsman Advanced Materials (CH).

*Corresponding author. Tel.: +41(0)585 882 620, e-mail: jakub.korbel@ch.abb.com.

Table 1. Overview of materials (fraction of every component is given in parts per hundred)

| Type | Commercial name | Supplier | Quantity |
|---|---|---|---|
| Epoxy resin | CY184 | Huntsman Advanced Materials (CH) | 100 phr |
| Anhydride hardener | HY1235 | Huntsman Advanced Materials (CH) | 90 phr |
| Catalyst | DY062 | Huntsman Advanced Materials (CH) | 0.5 phr |
| Silica filler | Silbond W12 EST | Quarzwerke (DE) | 354phr |

## 3. Measurements of the critical load of different designs of the flanges

The critical bending load was observed in five different designs of the flange (see Fig. 1). All flanges have an external diameter of 80 mm and a total length of 40 mm. The main difference in the design is the clamping diameter (40 mm for variants A, C, D and 30 mm for variants B and E) and the clamping angle ($90\,^\circ$ for variant A and B, $60\,^\circ$ for variant C, $30\,^\circ$ for D and $15\,^\circ$ for E). The flanges are composed of aluminum, which is approximately six times stiffer than the epoxy. This leads to a stress concentration in the contact zone.

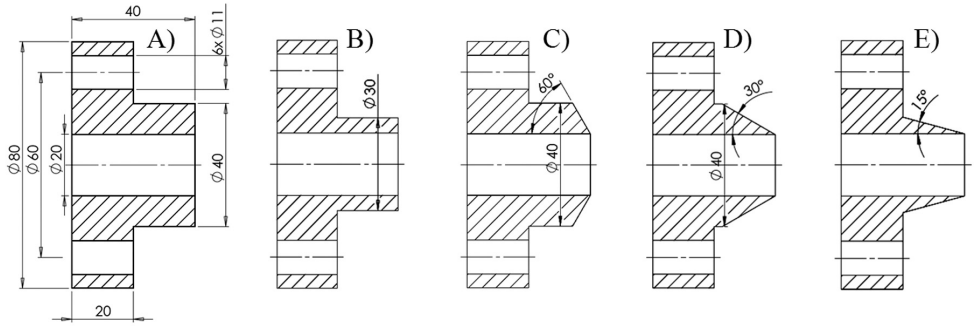


Fig. 1. Cross sections of the design variants of the flanges

The Aluminum flange was fixed using six steel bolts M10 to the mounting tool, which was constrained by two M20 bolts (see Fig. 2). The force was applied to the 250 mm long epoxy bar through the universal testing device Zwick and the force-displacement diagram was recorded until failure.

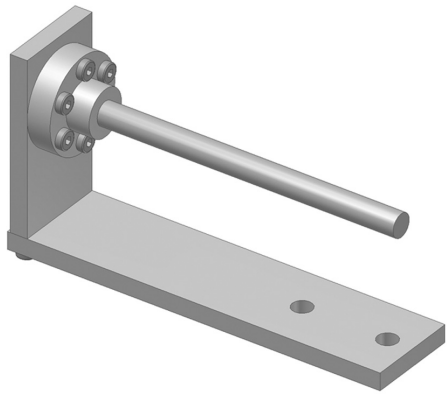

Fig. 2. Testing assembly

## 4. Fracture mechanical approach for determination of the failure load

The mismatch of mechanical properties (aluminum is several times stiffer than the adhesive and the epoxy resin) and sharp edge of the flange leads to a stress singularity in the vicinity of the interface. The stress based failure criterion cannot provide reasonable failure prediction; therefore the fracture mechanical approach must to be used. In our approach, singular stress concentrator is modeled as a bi-material notch (see Fig. 3) with a stress singularity exponent which differs from $1/2$. For specific configuration of glued flange, stress field distribution in the epoxy in influenced by the glue, therefore this very small layer (100 $\mu$m) has to be included.

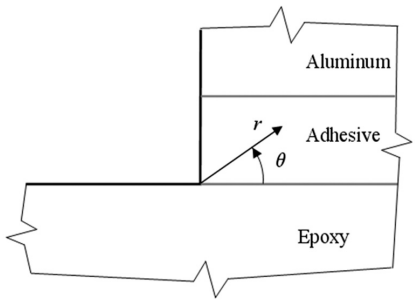


Fig. 3. Bi-material notch

The stress field distribution for the specific geometry of a bi-material notch is given by the following equation in terms of generalized stress intensity factors (GSIFs) $H_k$:

$$\sigma_{ijm} = \sum_{k=1}^{n} \frac{H_k}{\sqrt{2\pi}} \cdot r^{-p_k} \cdot F_{ijkm}(\theta, \text{geom}, m, \ldots), \tag{1}$$

where $n$ is the number of corresponding singular terms. For the example if the adhesive would be neglected, flanges with blunt angles ($90\,^\circ$ or $60\,^\circ$) would have two singular terms, corresponding to the two exponents $p_1$ and $p_2$, and the two GSIFs $H_1$, $H_2$. Flanges with sharp angles ($30\,^\circ$ or $15\,^\circ$) would have only one singular term. Because the adhesive was included, $90\,^\circ$ angle between the epoxy and the adhesive was considered, leading for all cases to two singular terms. $\sigma_{ijm}$ is defined as the stress tensor respecting the polar coordinates $i, j = r, \theta$, the subscript $m$ determines the materials (adhesive and epoxy resin) where the stresses are located, $F_{ijkm}$ calibrating functions and $r$ is the distance from the notch tip. Exponents of the stress singularities $p_k$ can be derived based on Dundur's parameters [3]. The calibrating functions $F_{ijkm}$ for the specific case of the bi-material notch can be computed from stress singularity exponents [1]

$$\begin{aligned}
F_{rrkm} &= (2-p_k)(-a_{mk}\sin((2-p_k)\theta) - b_{mk}\cos((2-p_k)\theta) + \\
&\quad 3c_{mk}\sin(-p_k\theta) + 3d_{mk}\cos(-p_k\theta)) \\
F_{\theta\theta km} &= (p_k^2 - 3p_k + 2)(a_{mk}\sin((2-p_k)\theta) + b_{mk}\cos((2-p_k)\theta) + \\
&\quad c_{mk}\sin(-p_k\theta) + d_{mk}\cos(-p_k\theta)) \\
F_{r\theta km} &= (2-p_k)(-a_{mk}\cos((2-p_k)\theta) + b_{mk}\sin((2-p_k)\theta) + \\
&\quad c_{mk}\cos(-p_k\theta) - d_{mk}\sin(-p_k\theta)).
\end{aligned}$$

The coefficients $a_{mk}$, $b_{mk}$, $c_{mk}$, $d_{mk}$ for $k = 1, 2$ are known parameters depending on the material combination and flange geometry, and they are normalized so that for the case of a

crack in a homogeneous material ($p_I = p_{II} = 0.5$) the GSIFs $H_1$ and $H_2$ corresponds to SIFs $K_I$ and $K_{II}$.

### 4.1. Generalized stress intensity factors and the limit values

Prediction of the rupture is based on one parameter fracture mechanics. For homogeneous materials, the most widely used approach is based on the stress intensity factor and its comparison with material parameter fracture toughness. The criterion of stability expression is written as follows:

$$K_I < K_{IC}. \tag{2}$$

Similarly, we can define the criterion for unstable crack propagation of a bi-material notch [2]:

$$H_k < H_{IC}\left(K_{IC}\right). \tag{3}$$

The values of GSIF $H_k$ can be obtained from finite element analysis (FEA) by direct method or integral approach. The limit value of the GSIF generalized fracture toughness $H_{IC}$ depends on the critical material characteristic $K_{IC}$. The maximum values of tangential stress (see Fig. 5) indicate that the fracture will propagate into the epoxy with angle $-73^\circ$ which nicely corresponds with measured values. For estimation of the generalized fracture toughness (GFT) the criterion based on mean values of tangential stress (MTS) was used and is defined by the following equation:

$$H_{1C} = \frac{2K_{IC}}{\dfrac{d^{0.5-p_1}}{1-p_1}F_{\theta\theta 1m}\left(\theta_0\right) + \Gamma_{21}\dfrac{d^{0.5-p_2}}{1-p_2}F_{\theta\theta 2m}\left(\theta_0\right)}, \tag{4}$$

where $\Gamma_{21}$ is a ration between GSIFs $H_2/H_1$, and $d$ is a micromechanical parameter which must to be chosen in dependence on the mechanism of rupture, see [1]. For easier representation of the results, critical bending force $F_{crit}$ can be derived:

$$F_{\text{crit}} = F_{\text{appl}}\frac{H_{IC}}{H_1\left(F_{\text{appl}}\right)}, \tag{5}$$

where $F_{\text{appl}}$ is the applied bending force used in numerical calculations of $H_1$ and $H_2$. Unstable crack propagation will not occur if the applied bending force is lower than the critical one:

$$F_{\text{appl}} < F_{\text{crit}}. \tag{6}$$

### 4.2. Numerical model

The stress field computation was carried out by the commercial FEM code Abaqus. The density of the mesh is shown on Fig. 4. Approximately 20 thousand, 20-node quadratic brick elements with refinement near singularity were used. Analysis was simplified by using one plane of the symmetry. Perfect adhesion between the flange, the adhesive and epoxy bar was assumed. The thickness of the adhesive was 100 $\mu$m. All degrees of freedom of the flange's holes were constrained in order to represent fixation by the bolts. The load was represented by a concentrated force of 100 N coupled to all nodes at the end of epoxy bar.

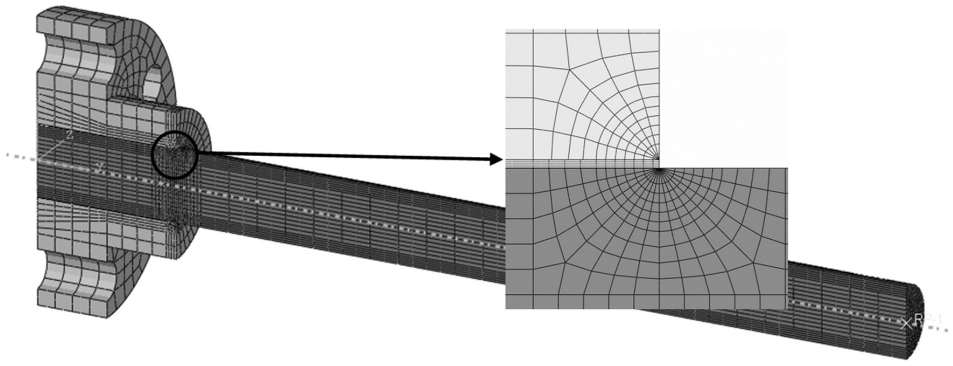

Fig. 4. Density of the mesh and detail of the interface

The material characteristics were taken as follows:

- Material 1 – aluminum – Young's modulus $E_1 = 70$ GPa, Poisson's ratio $\nu_1 = 0.3$, fracture toughness $K_{IC} = 24\ \mathrm{MPa} \cdot \mathrm{m}^{1/2}$.
- Material 2 – adhesive – Young's modulus $E_2 = 4.7$ GPa, Poisson's ration $\nu_2 = 0.34$, fracture toughness $K_{IC} = 2\ \mathrm{MPa} \cdot \mathrm{m}^{1/2}$.
- Material 3 – epoxy resin – Young's modulus $E_3 = 12$ GPa, Poisson's ratio $\nu_3 = 0.3$, fracture toughness $K_{IC} = 2.8\ \mathrm{MPa} \cdot \mathrm{m}^{1/2}$, Yield stress $\sigma_y = 92$ MPa.

### *4.3. Results*

The tangential stress around the notch tip (Fig. 5) with respect to the coordinate system shown on Fig. 3, determines the direction of the crack propagation. Maximal value can be found in the epoxy resin at the angle $-73°$. From the static stress field distribution it is also visible that the angle of maximal tangential stress changes from $-73°$ to $-90°$ which means that the crack should change direction during propagation and it was also observed in experiments.

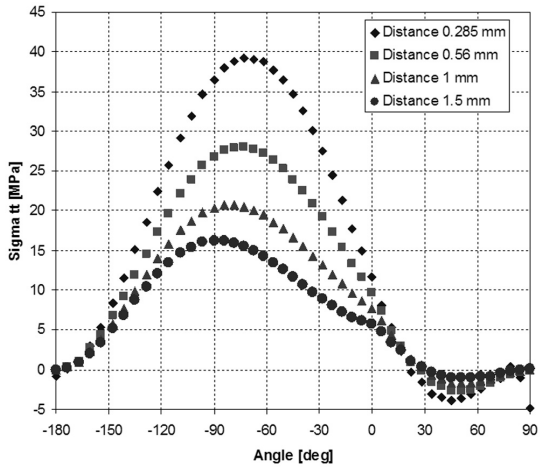


Fig. 5. Tangential stress around the interface

The actual angle of the crack propagation was measured by the device used for surface roughness measurements Mahr Perthometer Concept PGK (see Fig. 6). The profile of the fracture surface was recorded 1 mm from the internal fracture surface to the crack initiation location. Reasonable correspondence between the measurement ($-74.67°$) and the simulation ($-73°$) was found.

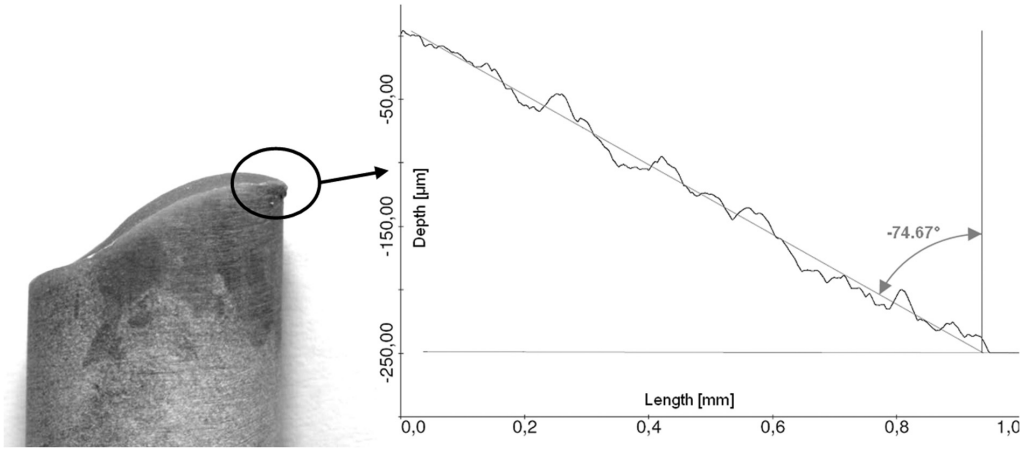


Fig. 6. Fracture surface and the angle of the propagation

For estimation of the GSIFs, the direct method was selected due to the simplicity. The method consists of extracting the tangential stresses from two independent paths oriented from the tip into the material (see Fig. 7) and using equation (1) for each single node on the path. Consequential extrapolation of the GSIFs values into the tip provides the desired values of $H_1$ and $H_2$. The interval of the extrapolation has to be selected carefully and results should not be influenced by the stress singularity, but should not be far from the tip. Correct lengths of the paths are characterized by linear continuance of GSIF values. The selection of the path's angle $\theta_1$ and $\theta_2$ is arbitrary, but one path should be selected at the angle with the highest tangential stress.

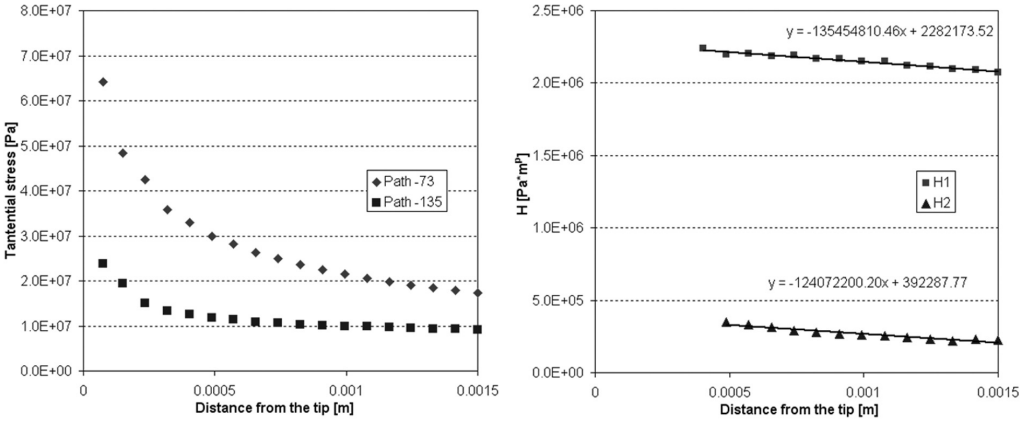


Fig. 7. Tangential stress and extrapolation of the GSIFs to the tip

GSIFs $H_1$ and $H_2$ and their critical values for all design variations of the flanges were calculated as well as the critical applied bending load according to equation (5). The results of the calculated critical bending force as a function of the parameter $d$ are shown on Fig. 8. This parameter reflects the mechanism of the rupture. For polycrystalline materials such as steel, value of parameter $d$ should be chosen in the range of 2–5 times the size of grains. For polymeric thermosetting materials the magnitude of the parameter $d$ has not been determined yet, therefore critical bending force is provided in as a reasonable range of the magnitude of the parameter $d$. However, possible way of determination of $d$ parameter can be found in the literature [4]:

$$d = \frac{1}{\pi}\left(\frac{K_{IC}}{\sigma_y}\right)^2. \tag{7}$$

The determination of the parameter $d$ is not in this case based on micromechanical parameters (grain size etc.), but it is derived from the fracture toughness and the yield stress of the epoxy resin. According equation (6) parameter $d$ should have value 300 $\mu$m. The comparison of the experimental data with the simulation is shown on Fig. 8. Minimal critical force was observed and predicted for initial design (diameter 40 mm) and maximal for the last design (diameter 30 mm, angle 15). This behavior was expected due to reduction of the stiffness of the flange in the location of the crack initiation, which should lead to lower stress concentration. If we consider $d$ parameter 300 $\mu$m, the biggest difference (15.2 %) can be found in case of flange with diameter 30 mm and angle $15°$. The disagreement between the simulation and the experiment can be caused by the preparation of the epoxy bar, which was machined in order to remove release agent and secure the assembling tolerances. Machined surface could be damaged and therefore the crack was initiated sooner than predicted.

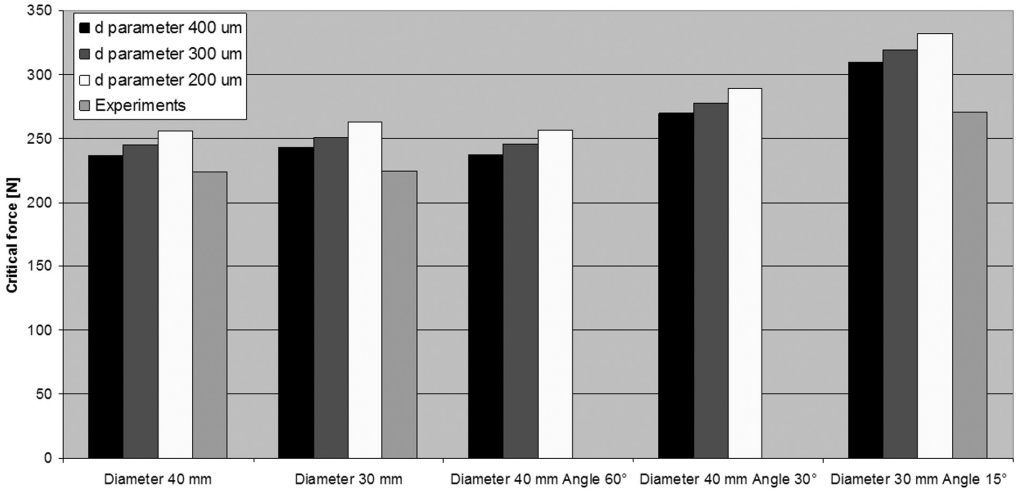


Fig. 8. Comparison of measured and calculated critical bending forces

## 5. Conclusion

Several design variations of aluminum-epoxy flanging loaded by bending force were experimentally investigated. The results were compared with numerical predictions of the failure. The fracture mechanical approach based on generalized stress intensity factors was employed and

limit value generalized fracture toughness was calculated by using mean tangential stress failure criterion. The comparison of measurements with simulations shows in the worst case scenario 15.2 % disagreement, which can be caused by the preparation of the epoxy bars. Across this disagreement, the approach provides correct estimation of the design improvements in terms of the maximal critical bending force applied on the structures with bi-material interfaces.

## Acknowledgements

The authors are grateful for financial support through the Research projects of the Academy of Sciences of the Czech Republic (1QS200410502 and AVOZ20410507) and the project of the Czech Science Foundation (101/08/0994).

## References

[1] Klusák, J., Knésl, Z., Náhlík, L., Crack initiation criteria for singular stress concentrations. Part II: Stability of sharp and bi-material notches. *Engineering MECHANICS*, 2007, Vol. 14, No. 6, p. 409–422.

[2] Knésl, Z., Klusák, J., Náhlík, L., Crack initiation criteria for singular stress concentrations. Part I: A universal assessment of singular stress concentrations. *Engineering MECHANICS*, 2007 Vol. 14, No. 6, p. 399–408.

[3] Qian, Z. Q., On the evaluation of wedge corner stress intensity factors of bi-material joints with surface tractions. *Computers and Structures*, 2001, 79 53–64.

[4] Taylor, D., The theory of critical distances. *Engineering Fracture Mechanics,* 2007, 75 1 696–1 705.